THE MASS, DECAY PROPERTIES, AND LEVELS OF ^{36}K FROM THE ^{36}Ar(p,n)^{36}K AND ^{36}Ar(^{3}He,t)^{36}K REACTIONS

by

DANIEL WILLIAM MILLER

A thesis submitted to the Graduate Faculty of
North Carolina State University at Raleigh
in partial fulfillment of the
requirements for the Degree of
Doctor of Philosophy

DEPARTMENT OF PHYSICS

RALEIGH

1971

APPROVED BY:

L. N. Ingraham D. R. Tilley

R. C. Bullock F. G. Everling
Chairman of Advisory Committee

BIOGRAPHY

The author was born April 6, 1939, in the town of Albemarle, North Carolina. He was reared and attended grammar school in both Albemarle and Rowan County, North Carolina. He graduated from Granite Quarry High School, Granite Quarry, North Carolina in 1957.

In 1961, the author received a Bachelor of Science degree with a major in nuclear engineering from North Carolina State University at Raleigh. The author was then employed by Pratt and Whitney Aircraft Company, East Hartford, Connecticut to investigate the technical feasibility of advanced electrical power systems.

He began his graduate study in physics at North Carolina State University at Raleigh in 1965, and received an appointment as a research assistant at the Triangle Universities Nuclear Laboratory (TUNL), Durham, North Carolina in 1967. He was permitted to pursue full-time research in experimental nuclear physics at TUNL.

The author married Miss Dorothy Prewitt Zola in 1963 and they have one child, Jonathan Paul, age three.

ACKNOWLEDGMENTS

The author wishes to express his sincere appreciation to the many people who have contributed inspiration, counsel, and assistance in the preparation of this study. The guidance and help of Professor F. G. Everling, Chairman of the Advisory Committee, is most gratefully appreciated. Sincerest gratitude is also extended to other members of the committee, Professors L. W. Seagondollar, D. R. Tilley, and R. C. Bullock, for their counsel and assistance.

A very special thanks is given to Drs. G. A. Bissinger and S. M. Shafroth of the University of North Carolina at Chapel Hill; Dr. A. A. Jaffe of Hebrew University, Jerusalem; Dr. T. G. Dzubay of Duke University; Dr. F. G. Everling and D. A. Outlaw of North Carolina State University at Raleigh, and Dr. T. A. White of Furman University, Greenville, South Carolina, all of whom were associated with the Triangle Universities Nuclear Laboratory (TUNL), for their essential help in planning and carrying out the experimental program. Gratitude is also extended to P. W. Tillman, Jr., R. O. Nelson, and C. E. Ragan, III for use of their computer programs.

Sincere appreciation is also given to Dr. H. W. Newson, Director of TUNL, and the entire laboratory staff for their valuable help and for the use of the facilities. A special thanks is extended to Dr. L. W. Seagondollar, Chairman of the Physics Department at North Carolina

State University at Raleigh, for his guidance and support. Gratitude is also expressed for the research assistantship which made the author's graduate study possible.

The work was supported by the U. S. Atomic Energy Commission.

Finally, the author wishes to express his thanks to his wife, Dorothy, for her patience and consideration during the course of this study, and for the many hours she spent in typing this thesis.

TABLE OF CONTENTS

TABLE OF CONTENTS (Continued)

TABLE OF CONTENTS (Continued)

LIST OF TABLES

LIST OF FIGURES

Page

1. INTRODUCTION

The goal of experimental nuclear physics is to gain quantitative knowledge of the observable characteristics of nuclei. This knowledge can then be used to develop and test the underlying concepts of nuclear structure. One useful area of research is to study the production and decay of radioactive isotopes. In this thesis, an investigation of the proton-rich nucleus ^{36}K is described.

Two quantities which are fundamental to the description of a radioactive isotope are its mass and half-life. At the outset of the present work, the mass of ^{36}K had been predicted by Kelson and Garvey (1966) and by Berg et al. (1967), but no direct determination had been reported in the published literature. Because of the precise energy resolution of the TUNL Cyclo-Graaff accelerator, accurate mass determinations can be made by measurements of reaction Q-values. In this report, the threshold for the $^{36}Ar(p,n)^{36}K$ reaction and the Q-value for the reaction $^{36}Ar(^3He,t)^{36}K$ are used to obtain the ^{36}K mass with a precision of $\pm$ 30 keV.

The half-life has been measured by observing the positron decay of ^{36}K to ^{36}Ar following production of ^{36}K by means of the $^{36}Ar(p,n)^{36}K$ reaction. This experiment was first performed by Berg et al. (1967), who also analyzed the resulting gamma-ray transitions in ^{36}Ar and identified the first T = 1 excited state in that nucleus. However, our measurement of the ^{36}K half-life resulted in a new value which is 30%

higher than that previously reported. This difference led to contradictions with the theory and systematics of beta decay. The resolution of these contradictions required a complete repetition of the Berg experiment in which improvements in gamma-ray energy and intensity measurements were made.

Another important part of the study of a radioactive isotope is knowledge pertaining to its formation. In this thesis the ^{36}K yield from the $^{36}Ar(p,n)^{36}K$ reaction is studied as a function of proton energy from threshold to 30 MeV. The shape of the excitation curve provides information about the optimum proton energy for ^{36}K production as well as important information about nuclear structure such as compound nuclear resonance effects.

Finally, an investigation of the excited states of ^{36}K by means of the $^{36}Ar(^{3}He,t)^{36}K$ reaction is described. The energies of these states are of special interest because the levels are members of T = 1 triplets. These energies along with the ground-state mass are of particular significance since they complete measurements of the masses of all the $T_z = \pm 1$ nuclides up to and including mass 42.

2. REVIEW OF THE LITERATURE

2.1 Mass and Half-Life of ^{36}K

At the time this work began, two research groups had predicted the mass of ^{36}K but no measurement had been published. The first group, Kelson and Garvey (1966), used the assumption of charge symmetry of nuclear forces to develop a parameterless equation for the masses of proton-rich nuclei. Their prediction for the mass excess of ^{36}K is -17.42 ± 0.05 MeV. The second mass prediction was by Berg et al. (1967). They analyzed gamma transitions in ^{36}Ar following the positron decay of ^{36}K produced by the $^{36}Ar(p,n)^{36}K$ reaction. By this technique, a superallowed positron branch was found which led to the identification of the first $T = 1$ state in ^{36}Ar. By using the excitation energy of this state and an estimate of the Coulomb-displacement energy, the ^{36}K - ^{36}Ar mass difference was estimated to be 12.90 MeV. This leads to a ^{36}K mass excess of -17.33 MeV using the ^{36}Ar mass excess of -30.2305 ± 0.0011 MeV from the table of Wapstra and Gove (1971)[1].

Only one reference to a measurement of the ^{36}K mass has been found. This appeared in the unpublished literature and consisted of a Q-value measurement of the $^{36}Ar(^3He,t)^{36}K$ reaction by Matlock (1965).

---

[1] To be published in Nuclear Data Tables 9:265-468

This measurement resulted in a value for the ^{36}K mass excess of -15.58 MeV which does not agree with predictions or systematics.

The half-life of ^{36}K was also measured by Berg et al. (1967) in the experiment described above. By analyzing the time decay of the intensities of gamma transitions in ^{36}Ar, they found the ^{36}K half-life to be 0.265 ± 0.025 s.

2.2 Energy Levels of ^{36}K

Prior to the present work, no energy levels for excited states in ^{36}K had been measured. However, the general features of the ^{36}K level structure can be inferred from the analog nucleus ^{36}Cl. The level energies, spins, and parities of states in ^{36}Cl are summarized by Endt and van der Leun (1967).

2.3 Gamma Transitions in ^{36}Ar

The positron decay of ^{36}K to ^{36}Ar was first studied by Berg et al. (1967). They produced ^{36}K by means of the $^{36}Ar(p,n)^{36}K$ reaction using a 22-MeV proton beam which was turned on and off with a repetition period of about 1.5 s per cycle. During the beam-off portion of the cycle (0.75 s), a 3 cc Ge(Li) detector was used to accumulate three timed gamma spectra at 0.25 s intervals. From these spectra, they were able to identify six gamma rays originating from transitions in ^{36}Ar. The relative intensities of these gamma rays were then used to obtain positron branching ratios for the states populated. Log ft values

were calculated for each branch resulting in the identification of a superallowed transition to a state which must be the first T = 1 level in ^{36}Ar. Gamma-ray energy determinations were made and used to measure four ^{36}Ar level energies. The results of gamma-ray de-excitation following other reactions are summarized by Endt and van der Leun (1967).

3. EXPERIMENTAL EQUIPMENT

3.1 General Laboratory Description

The work described in this thesis was performed at the Triangle Universities Nuclear Laboratory which is jointly operated by N.C. State University, Duke University, and the University of North Carolina at Chapel Hill. Charged particle beams are produced by means of a Cyclo-Graaff accelerator. This machine consists of a 15-inch cyclotron which injects 15-MeV negative hydrogen ions into an F N tandem Van de Graaff accelerator. For proton energies below 15 MeV and for accelerating other particles such as ^{3}He, the Van de Graaff is used alone. Thus, these machines are capable of producing proton beams up to 30 MeV and helium beams up to 22 MeV while maintaining the precise energy control inherent in Van de Graaff accelerators.

The laboratory also contains a complete computing facility. A Honeywell DDP-224 computer is used for on-line data acquisition and for computer control of experimental equipment. An identical computer, except for memory capacity, is used for off-line data analysis. Peripheral equipment which is interfaced to the computers include typewriters, a paper tape read/punch unit, magnetic tape units, line printer, card reader, card punch, and display scopes equipped with light pens.

A floor plan of the laboratory appears in Figure 3.1.

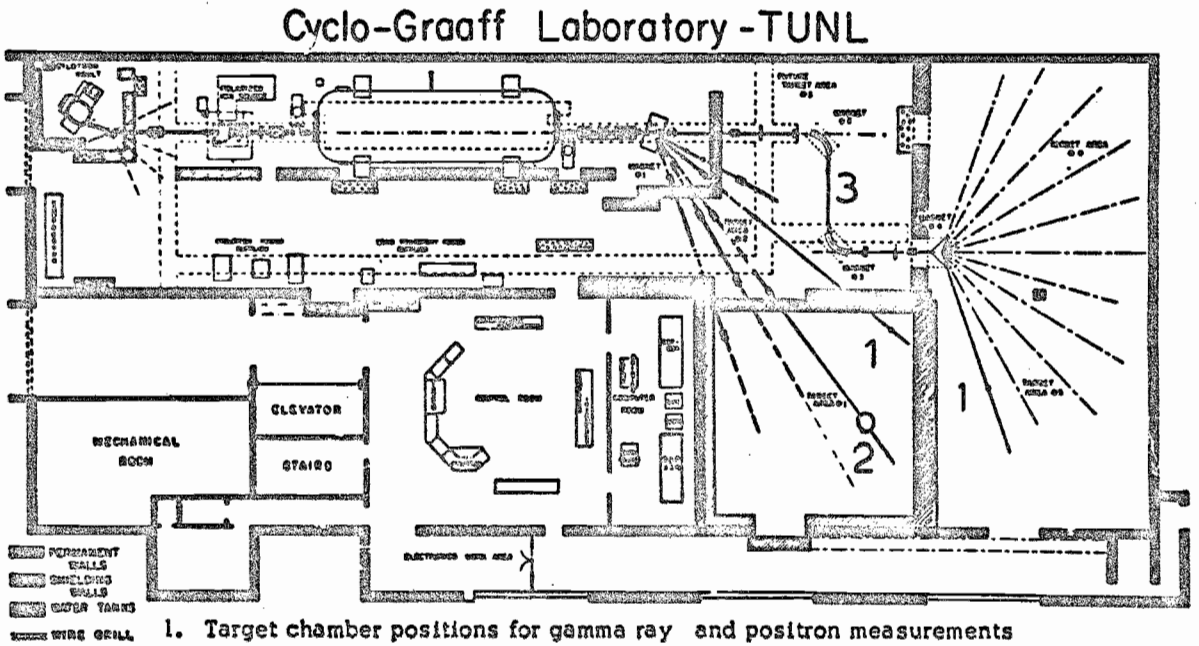

1. Target chamber positions for gamma ray and positron measurements
2. Scattering chamber
3. High resolution beam analyzing magnets

Figure 3.1 Laboratory floor plan

3.2 Beam Transport Systems

In this section, the magnetic and electrostatic devices which steer and focus the beam as well as special equipment such as the beam choppers will be described. Several target chambers and beam lines were used throughout the course of the experimental work. The beam was magnetically deflected into each of these target areas by setting the proper field in a bending magnet located after the accelerator. The beam is steered by an electrostatic deflector and focused by a magnetic quadrupole lens before entering the bending magnet.

3.2.1 Systems Using the Mechanical Chopper

For the mass and half-life determinations, the $^{36}Ar(p,n)^{36}K$ excitation curve above 15 MeV, and the gamma-ray measurements, a beam line located at a deflection angle of 38 degrees was used. The beam energy was stabilized by means of a corona control circuit using feedback signals taken from beam slits located after the deflection magnet.

Following the control slits, a mechanical chopper was placed in the beam line. This device operated by rotating a slotted cylinder in the path of the beam. For the earlier experiments which include the mass and half-life determinations and the excitation curve above 15 MeV, the width of the slot was chosen to give a beam-off time equal to twice the beam-on time. Cams placed on the shaft of the rotating cylinder were used to operate micro-switches which activated an electronic

pulse generating circuit. The cam lobes were placed so that a pulse was generated and sent to the computer each time the beam was interrupted. The computer used these pulses to control the acquisition of data from the detectors. For the gamma-ray measurements a new chopper cylinder was installed which had a slot width selected so that the ratio of beam-on time to beam-off time was one to four. In addition, improvements were made in the chopper pulse generating system. In the new system, a cylinder was placed on the end of the rotating chopper shaft replacing the cams and micro-switches. Light passing through a small hole drilled through the center of the cylinder perpendicular to the axis activated a photodiode pulse generating circuit. The chopper was turned by a variable speed electric motor.

After the chopper, the beam line passed through two shielding walls before entering the target room. These shielding walls served to minimize background radiation which otherwise would have reached the detectors from the chopper during the beam-off counting periods. After passing through the target chamber, the beam was stopped in a thick carbon block approximately six feet away from the detectors. Concrete, paraffin and lead shielding were placed around the detectors and the end of the beam pipe. This shielding protected the Ge(Li) detector from neutron damage during the beam-on activation periods and reduced background radiation during the counting periods. Two magnetic quadrupole lenses and a magnetic steerer were placed between the chopper and the

target chamber for focusing and steering the beam into the chamber. In addition, a double tantalum collimator with a 1/8-inch diameter circular aperture upstream followed by a 3/16-inch aperture two inches away was placed 12 inches from the target. A quartz viewer was located in front of this collimator which could be moved into and out of the beam by remote control. The beam spot on the quartz viewer was viewed by closed-circuit television and served as a valuable aid in focusing and steering the beam.

3.2.2 System Used for the $^{36}Ar(^{3}He,t)^{36}K$ Reaction

For the $^{36}Ar(^{3}He,t)^{36}K$ experiment, the ^{3}He beam was deflected 58 degrees into a beam line which connects to a scattering chamber. As for the 38 degree beam line described above, the control slits for the corona discharge of the Van de Graaff generator are located after the magnet, and two shielding walls separate the magnet from the target chamber. Two magnetic quadrupole focusing lenses are used for beam focusing and a magnetic steerer is also located on the beam line. Beam collimation is achieved by a special system located inside the scattering chamber. Tantalum bars which are electrically insulated from each other form a variable size rectangular aperture. Currents which are a result of beam striking the collimator bars provide feedback signals to a circuit that automatically activates the magnetic steerer and thus keeps the beam centered through the collimator. After passing through

the scattering chamber, the beam is stopped 15 feet away in the center of a water tank which is four feet in diameter.

3.2.3 High Resolution Magnetic Analyzer

Toward the end of the experimental work a newly developed magnetic analyzing system became available. This system has the advantage of very precise beam energy resolution and was used to investigate the $^{36}Ar(p,n)^{36}K$ excitation curve below 15 MeV. In this experiment, the ^{36}K yield was measured by observing the amount of positron activity having the time-decay characteristic of ^{36}K. The beam was chopped by applying a 25 kV potential across the vertical plates of the electrostatic steerer located just after the Van de Graaff accelerator. Application of the deflection voltage was controlled by a circuit which received signals from the computer.

After passing straight through the bending magnet which was used for the other experiments, the beam was dispersed somewhat in the horizontal direction by a magnetic quadrupole singlet focusing lense. This dispersion increases the sensitivity of the magnetic analyzing system. The beam then passed through two 90-degree bending magnets which allow only those protons whose energy is very close to the desired value to be transmitted. The slits which feed back current to the corona discharge control system were located between the two 90-degree magnets. After emerging from the magnetic analyzing system,

the beam was deflected 70 degrees by another bending magnet into the target chamber. A magnetic quadrupole focusing lens and a magnetic steerer were located between the 70-degree bending magnet and the target chamber.

3.3 Target Chambers and Gas Target Cells

3.3.1 Chamber for Gamma and Positron Measurements

The target chamber which was used for the gamma and positron measurements consisted of a vertical brass cylinder two inches in diameter intersecting a two-inch diameter horizontal cylinder through which the beam passed. The gas target cell was centered at the intersection and connected to the external target gas supply by means of a 1/16-inch copper tube which passes through the top of the chamber. Vacuum was maintained by a two-inch oil diffusion pump and water-cooled baffle connected to the bottom of the chamber. For both the gamma and positron experiments, the detectors were placed at an angle of 90 degrees with respect to the beam direction. To minimize the attenuation of the positrons, the radiation was detected through a thin mylar window located in the side of the chamber.

3.3.2 Scattering Chamber

A 23-inch diameter scattering chamber was used for the $^{36}Ar(^{3}He,t)^{36}K$ experiment. The detectors and their collimators were

mounted on a Freon-cooled track directed toward the center of the chamber. The track is connected to a movable plate in the bottom of the chamber which allows the detector angle to be changed without affecting the vacuum. The gas target cell was mounted in the bottom of the chamber and connected to the target gas supply by means of a copper tube. A turbo-pump was used to maintain the scattering chamber vacuum.

3.3.3 Gas Target Cells

The gas targets for the positron counting experiments and the $^{36}Ar(^{3}He,t)^{36}K$ reaction were contained in cylindrical cells situated vertically in the target chambers. The cell for the positron work was sealed by tantalum foil 0.00025 inches thick. Havar foil (43% Co, 18% Fe, 20% Cr, 13% Ni, 3% W, 3% Mo, Mn, C, Be) of the same thickness was used for the (^{3}He,t) experiment.

The gas cell for the gamma ray work was designed to give greater target thickness for a given amount of gas. This cell was a cylinder five inches long and 1/2 inch in diameter with the beam path along the axis. To minimize background activity, the ends of the cell were sealed with 0.001 inch thick DuPont Kapton, a high-temperature resistant plastic. Background was also reduced by lining the inside walls of the cell with several layers of 0.001-inch thick tantalum foil. This kept scattered protons from reaching the brass walls of the target cell.

A diagram of each gas cell is given in Figure 3.2.

3.4 Computer Systems

The laboratory computing system uses two Honeywell DDP 224 computers. One computer is used for data taking and analysis, and the second computer is used for data analysis only.

3.4.1 Data-Taking Computer

This machine has a memory capacity of 16,000, 24 bit words, and a computation speed of 1.9 μs for addition. The computer is interfaced to the following input-output devices: paper tape reader/punch, typewriter, card reader, line printer, two magnetic tape units, two display scopes with light pens, and several data input channels. In addition, the computer can be programmed to produce output pulses which can be used to control experimental equipment. The computer operates normally in a time-sharing mode which permits the running of two programs simultaneously. Computer interrupts with 32 priority levels are used to control operations.

3.4.2 Data Analysis Computer

The data analysis computer has a memory capacity of 8000 words and includes the built-in capacity for floating-point arithmetic. This machine has its own magnetic tape unit, typewriter, display scope and light pen, and is interfaced to a standard IBM keypunch machine for

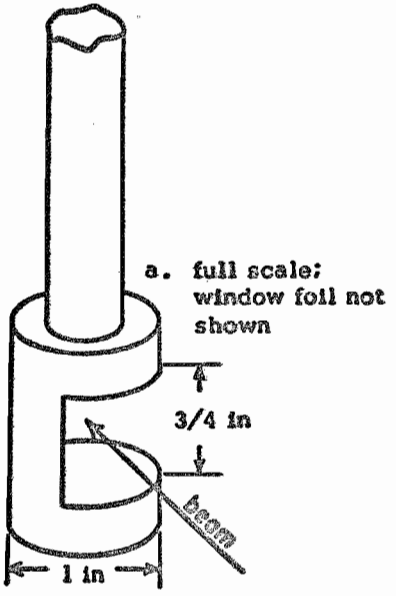

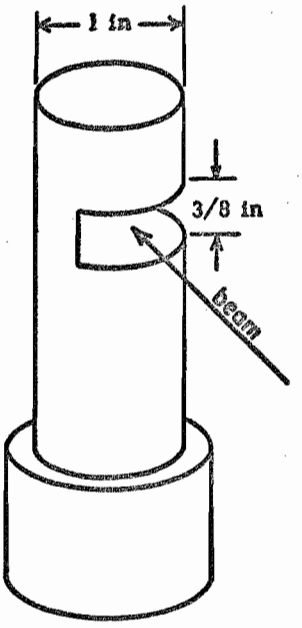

c. full scale; window foil not shown

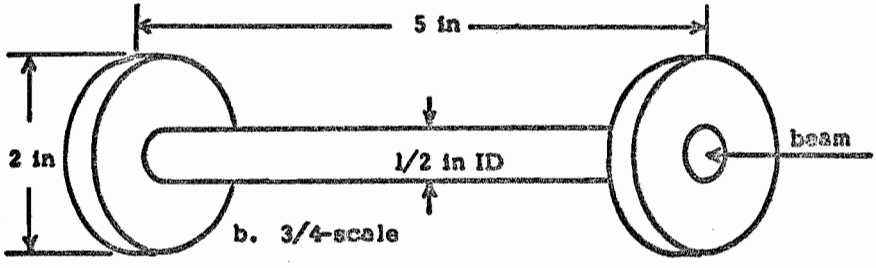

a. Cell for positron measurements
b. Cell for gamma-ray measurements
c. Cell for $^{36}Ar(^{3}He,t)^{36}K$ reaction

Figure 3.2 Gas target cells

punched card output. The data analysis computer shares the line printer, card reader, and paper tape read/punch unit with the other computer.

3.5 Detectors and Electronics

3.5.1 Positron Detector

A cylindrical plastic scintillator 5 cm in diameter and 4 cm thick was used as a positron detector. The scintillator was mounted on the face of a RCA model 6810A photomultiplier tube which was operated with a bias of -2200 volts. The phototube base was wired so that output signals were taken from the anode.

Pulses from the detector were then processed by a preamplifier, linear amplifier, and analog-to-digital converter. A pulser was connected to the test-pulse input of the preamplifier. This unit was calibrated by adjusting the calibration control until the pulse height at the output of the linear amplifier matched the amplitude of detector pulses from a radioactive source. Consequently, due to the linearity of the pulse generator, detector pulses of any energy could be simulated as an aid in checking and adjusting the detector electronics. A block diagram for the entire system is shown below in Figure 3.3.

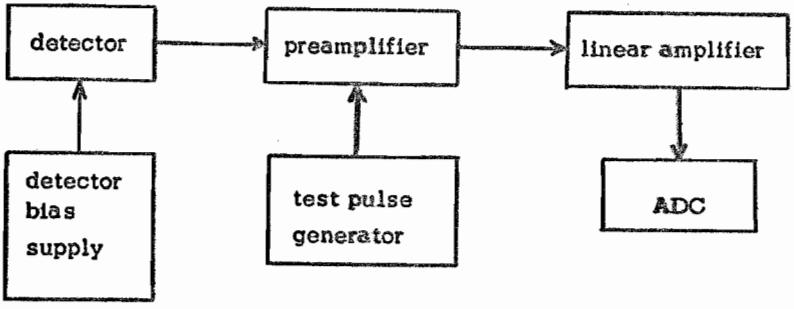

Figure 3.3 Positron detector electronics block diagram

3.5.2 Gamma-Ray Detector

An 80 cc Ge(Li) detector manufactured by Princeton Gamma-Tech Corporation was used for the gamma-ray measurements. A detector bias of -2000 volts was used. Pulses from the detector went to a pre-amplifier, linear amplifier, and an analog-to-digital converter before being processed by the computer.

3.5.3 Particle Identification Electronics

For the $^{36}Ar(^{3}He,t)^{36}K$ experiments, in which the tritons were detected, some technique had to be used for distinguishing the tritons from the other reaction products which include protons, deuterons, alpha particles, and scattered ^{3}He particles. To accomplish this, a system known as a telescope particle identifier was used. This device

consists of a pair of solid state detectors arranged so that particles pass through the first and are stopped in the second. Particle identification was achieved by a method first developed by Goulding et al. (1964) which makes use of differences in the rate of energy loss for different particles passing through an absorber. Specifically, if ΔE and E represent energy losses in the first and second detector, respectively, then it is known empirically that the expression $(E + \Delta E)^{1.76} - E^{1.76}$ has a different, energy-independent value for different types of particles. For the $^{36}Ar(^{3}He,t)^{36}K$ experiment signals occuring simultaneously in the ΔE and E detectors were amplified with precisely the same gain and summed to provide $E + \Delta E$ and ΔE inputs for the computer. The computer then used this information to identify the detected particle and store a count in the proper channel of the energy spectrum corresponding to the particle type. The details of the electronic setup are shown in Figure 3.4, and the computer program is described in Section 3.6.2.

3.6 Computer Programs for Data Taking

3.6.1 Chopped Beam Experiments

For experiments involving the chopper, a typical procedure takes the form of a repetitive cycle consisting of a beam-on activation period followed by a beam-off counting period. For measuring radiation produced from the decay of ^{36}K, the cycle time is of the order of one

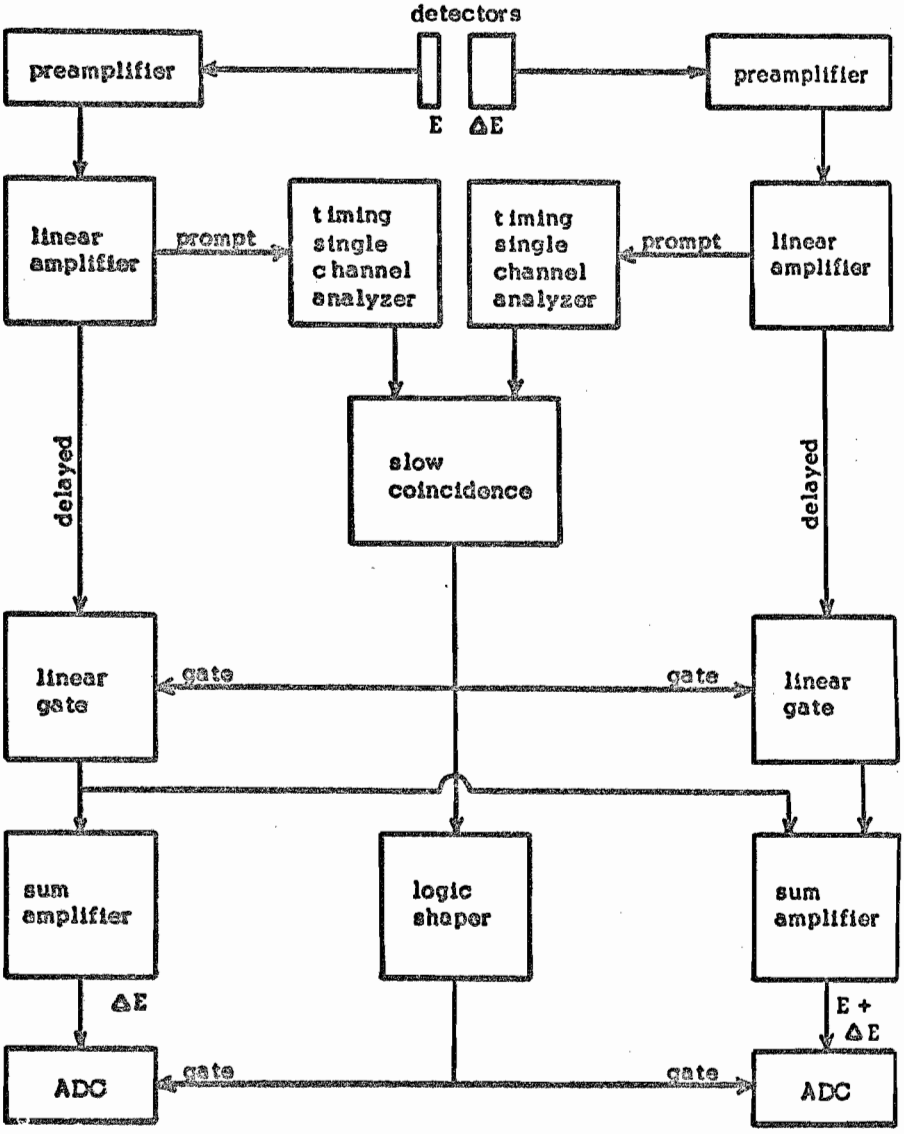

Figure 3.4 Particle identification electronics block diagram

second. During the beam-off period it is advantageous to accumulate separate spectra at precisely timed intervals, thus acquiring knowledge of the energy distribution and the time behavior of the measured radiation. To accomplish this, a computer program was written which used signals from the chopper and signals from a suitable timer such as a 60 Hz pulse generator to control the data acquisition. The computer program cycle begins when a pulse is received from the chopper indicating that the beam has been turned on. The computer then waits with the data input turned off for a specified number of timing pulses to allow for target activation. At the end of this period, data is allowed to accumulate in a certain block of computer memory for a specified time interval. At the end of that interval, data accumulation begins in another memory block. This process is repeated until either data acquisition is complete for all data blocks or a chopper signal is received. With the advent of a chopper signal, a new cycle begins.

The target activation time and the counting time per block are variable input items. These are set by the experimenter to be compatible with the chopper rotation speed and the number of data blocks. The total number of memory locations allocated for data storage is fixed. However, the operator may choose the number of timed blocks into which the total memory space is divided.

Another feature of the program is the option of computing the sums of counts over a specified range of channels for each time block. This

group of sums as well as the logarithm of the sums can be shown on the display scope or printed on the line printer. This gives the experimenter information about the intensity of detected radiation as a function of time for any energy interval of the spectrum.

Input-output features of the program include magnetic tape read/write, data display on the scope, and line printer output.

The program was modified somewhat for use with the electrostatic chopper which was used for the $^{36}Ar(p,n)^{36}K$ excitation curve between threshold and 15 MeV. For this version of the program, the computer sent out signals to control the chopper rather than receiving pulses from the chopper. This arrangement had the advantage of greater timing versatility because the ratio of beam-on to beam-off time was controlled by the experimenter rather than being fixed by the geometry of the rotating chopper.

3.6.2 Particle Identification Experiment

For the $^{36}Ar(^{3}He,t)^{36}K$ experiment a computer program was used which was written specifically for the particle identifier system described in Section 3.5.3. In that system, each detected event produces a pair of simultaneous signals which are analyzed by analog-to-digital converters and processed by the computer. One signal is proportional to the energy of the detected particle, and the other is proportional to the energy lost in the transmission detector. The computer uses these

inputs to compute the value of a particle identification variable which has a magnitude characteristic of the type of particle detected, i.e. proton, deuteron, triton, ^{3}He, or alpha. The program has two basic operating modes, the "mass mode" and the "energy mode". In the mass mode, the particle identification variable is stored in the memory and displayed on the computer display scope. This data is known as the "mass spectrum", and consists of peaks having areas proportional to the number of particles detected, and positions characteristic of the type of particle. The program operator picks out pairs of channel numbers called "mass windows", which correspond to the peak limits, and this information is read into the computer.

The energy mode is used for normal data taking. In this mode the computer compares the magnitude of the particle identification variable for each detected event with the limits of each mass window set from the mass spectrum. If the particle identification variable falls within a mass window, a count is added to the spectrum corresponding to that window in a channel number corresponding to the amplitude of the full-energy signal. Thus, a spectrum is accumulated for each type of particle for which a mass window was set. The program has the capacity for storing four 1024-channel spectra.

Input-output features of the program include magnetic tape read/write, line printer data listing, and data display scope.

4. EXPERIMENTAL PROCEDURES AND RESULTS

The positron activity produced when ^{36}K decays to ^{36}Ar following the $^{36}Ar(p,n)^{36}K$ reaction was used to measure the ^{36}K mass and half-life, as well as the ^{36}K yield. The positron detector used in each case was a cylindrical plastic scintillator 4 cm thick and 5 cm in diameter located approximately two inches from the target at an angle of 90 degrees to the beam direction. The same reaction was used to produce ^{36}K for gamma-ray measurements. For each experiment, an activation time of one or two half-lives followed by a counting time of several half-lives was achieved by chopping the beam. The level energies of excited states in ^{36}K were measured by detecting tritons from the $^{36}Ar(^3He,t)^{36}K$ reaction. The argon targets consisted of 99.9% ^{36}Ar at a pressure of 1/2 atm for the (p,n) reaction and 0.2 atm for the $(^3He,t)$ reaction.

4.1 Half-Life of ^{36}K and $^{36}Ar(p,n)^{36}K$ Yield from 15 MeV to 30 MeV

The half-life of ^{36}K had been previously measured by Berg *et al.* (1967) to be 0.265 ± 0.025 s. Therefore, when the present work began, the primary interest was in measuring the ^{36}K mass, investigating the $^{36}Ar(p,n)^{36}K$ yield, and searching for ^{35}K via the $^{36}Ar(p,2n)^{35}K$ reaction. However, a half-life measurement was an essential byproduct of the experimental procedure. Thus, when preliminary work indicated

a discrepancy of about 30% in the previously published value, a careful remeasurement of the half-life was performed.

4.1.1 Experimental Procedure

The basic concept of the procedure was to identify positrons arising from the decay of ^{36}K by their energy and decay time. This was accomplished with an automated procedure using an on-line computer which was programmed to accumulate separate energy spectra at precisely timed intervals in synchronization with the beam chopper.

The half-life and the beta end-point energies for several positron decay branches were fairly well known from the work of Berg et al. (1967). They found from gamma-ray measurements and a prediction of the ^{36}Ar - ^{36}K mass difference that positron branches with end-point energies of 5.27 MeV (25%), 7.44 MeV (5%), and 9.91 MeV (70%) should be present. This information was used to select the chopper rotation speed and the amplifier gain.

A test-pulse generator was used to check out and adjust the electronics. Because Compton scattering can be detected by a plastic scintillator, the pulser was calibrated by adjusting the calibration control until test pulses corresponding to a 1 MeV pulser setting were stored in the same computer memory channel as the Compton edge from a ^{60}Co gamma-ray source. The pulser was then used to adjust the gain of the linear amplifier so that beta particles ranging in energy from 0 to

10 MeV could be detected. The rotational speed of the mechanical beam chopper was adjusted to obtain a beam-off counting period of about two seconds, or approximately six half-lives. Because of the geometry of the chopper, this rotation speed resulted in a target activation time of about one second.

Input to the data-taking computer program was chosen so that the total memory space of 2048 channels was divided into 32 blocks of 64 channels each. The program timing was regulated so that data was allowed to accumulate in each memory block for precisely 0.10 s. The computer timing signals were generated by a 60 Hz pulser.

In order to measure the half-life accurately, the relative detector dead time for spectra taken in different time blocks had to be considered. This was done by storing counts from the pulser in the high-energy portion of the spectra where very few real counts occur. Since these pulses are generated at a constant rate, the relative number which are stored in each spectrum can be used to find the relative dead time.

Proton beams for this experiment were produced by the Cyclo-Graaff accelerator. The beam energy was varied in steps over the 16.5 MeV to 30 MeV energy range of the accelerator so that the relative yield of the $^{36}Ar(p,n)^{36}K$ reaction could be measured. First, the proton energy was varied from 17 MeV to 30 MeV in steps of 1 MeV. Then, the beam energy was reduced in steps of 1 MeV from 29.5 MeV to 16.5 MeV.

The Van de Graaff generator was then turned off to obtain a point at 15.2 MeV using the cyclotron alone. Thus, the reaction yield was measured from about 15 MeV to 30 MeV at 1/2-MeV intervals. The beam intensity was typically about 60 nA, and the total collected charge for points on the yield curve varied from 4 to 16 μC.

An understanding of the background activity is important for determining the ^{36}K half-life and for evaluating the reaction yield. For this study, data was taken at an incident proton energy of 29.5 MeV with the target gas removed from the gas cell. Thus, the energy distribution and the time decay of the background activity was determined. In addition, an experiment was performed at 18.5 MeV using the argon target and a chopper rotation speed which was decreased to 1/2 the normal value. Data was accumulated in each time block for 0.20 s giving a total counting time per chopper cycle of about four seconds, or twelve half-lives. In this way, the long-lived background activity remaining after most of the ^{36}K had disappeared could be studied.

4.1.2 Data Analysis and Results

The data was analyzed with the help of a computer program written specifically to handle information that was recorded on magnetic tape by the data-taking program. The off-line computer was used for this work. The data-analysis program has the capability of reading the beta spectra from tape and displaying them on the computer scope. A decay

curve can then be generated for any beta energy range by summing the data in adjacent channels between specified limits in each of the timed spectra. This decay curve can then be fitted by least-squares analysis to the theoretical function

$$Y = A_1 \exp(-\ln(2)t/T_1) + A_2 \exp(-\ln(2)t/T_2) + A_3$$

where Y is the yield at time t, A_1 is the amplitude parameter for a decaying component with half-life T_1, A_2 is the amplitude parameter of a second component with half-life T_2, and A_3 is the amplitude of a constant background component. One or two of the amplitude parameters can be set equal to zero if the data is believed to consist of fewer than three components. In addition, any combination of the amplitude and half-life parameters can be held fixed while optimizing the fit with respect to the remaining variable parameters. The data comprising the decay curve, the final fit to this data, and the parameters along with their uncertainties can then be printed on the line printer. The data for each incident proton energy was fitted with a function consisting of one decay-component plus a constant background. The half-life was held fixed at a value obtained by a rough, preliminary analysis, and the amplitude parameters were allowed to vary. By comparing these results, it was found that a peak in the ^{36}K yield occurred at proton bombarding energies between 16.5 MeV and 18.5 MeV. Therefore, for the final half-life measurement beta spectra taken with proton energies of 16.5, 17.0,

17.5, 18.0, and 18.5 MeV were summed together in order to improve the statistics.

The beta spectrum sum limits which generate the decay curve had to be carefully selected so that any systematic variation in the decay rate of particular energy regions of the beta spectra could be avoided. Therefore, a study was made which determined the decay rate of each channel of the timed spectra. The results of this study appear in Figure 4.1 where the half-life is plotted as a function of channel number. This figure shows that the low energy portion of the beta activity contains long-lived background components which should be excluded by the sum limits. Using Figure 4.1 as a guide, channels 23 through 43 were selected to generate the decay curve for the half-life determination. This corresponds to a beta energy range of about 3.8 MeV to 6.8 MeV. The upper limit was chosen to avoid counts from the pulser peak which was included for dead-time correction. The timed positron spectrum which was used to obtain the first decay curve point is also plotted in Figure 4.1.

In order to determine the nature of the background activity, two experimental procedures were used. In the first, a constant background of 28 ± 3 counts in the sum of channels 23 through 43 was obtained from data taken with the argon removed from the target cell. An incident proton energy of 29.5 MeV was used for this experiment. In the second procedure, the argon target was used but the time allowed for each beta

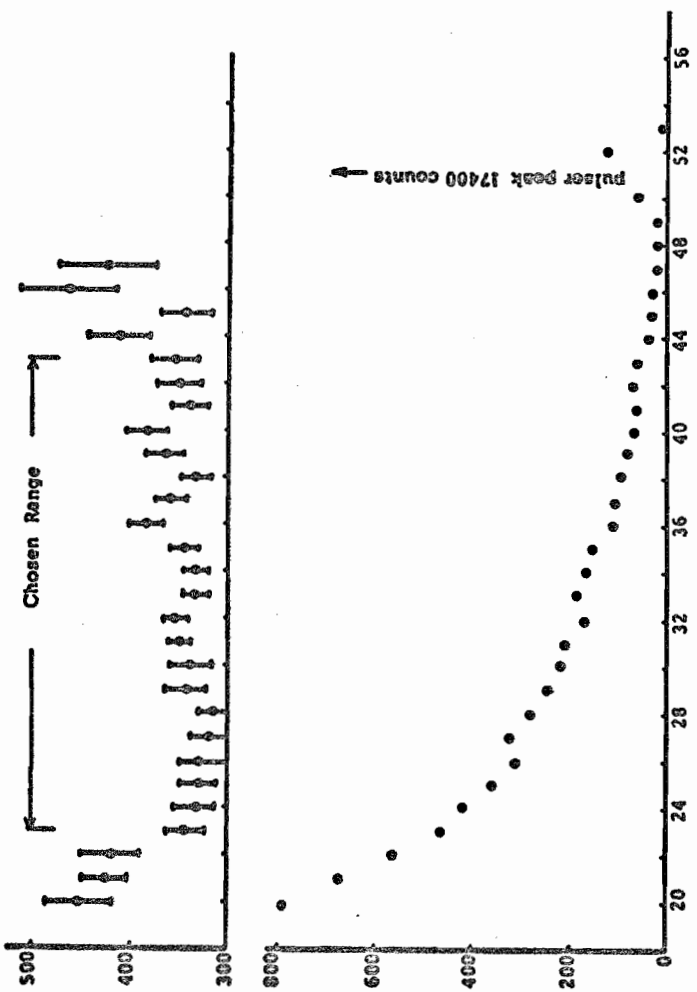

Figure 4.1 Time decay of each channel in the positron spectrum (upper) and typical positron spectrum (lower)

spectrum to accumulate was increased from 0.10 s to 0.20 s and the chopper speed cut by half. Analysis of this data shows that the activity levels off to a constant background of 26 $\pm$ 3 counts per 0.10 s time interval using the same sum limits.

The final result of the half-life measurement using timed beta spectra which were the sum of five groups of data taken with different bombarding energy is 0.341 $\pm$ 0.006 s. The best fit was obtained with a constant background of five times 24 counts which is in good agreement with the independent background determinations. The decay curve and fit are plotted in Figure 4.2.

Once the half-life was established, the data for each incident proton energy was analyzed keeping the half-life fixed. Consequently, the curve showing the relative yield of the $^{36}Ar(p,n)^{36}K$ reaction was obtained by plotting the amplitude parameters normalized with respect to collected charge as a function of energy. This curve is presented in Figure 4.3.

4.1.3 Search for ^{35}K

The mass of ^{35}K has been predicted by Kelson and Garvey (1966). If their prediction is correct, ^{35}K should be stable against proton emission and therefore be a positron emitter. Using this mass prediction, the threshold for the $^{36}Ar(p,2n)^{35}K$ reaction should be about 28.5 MeV. Therefore, positron spectra for proton energies above this

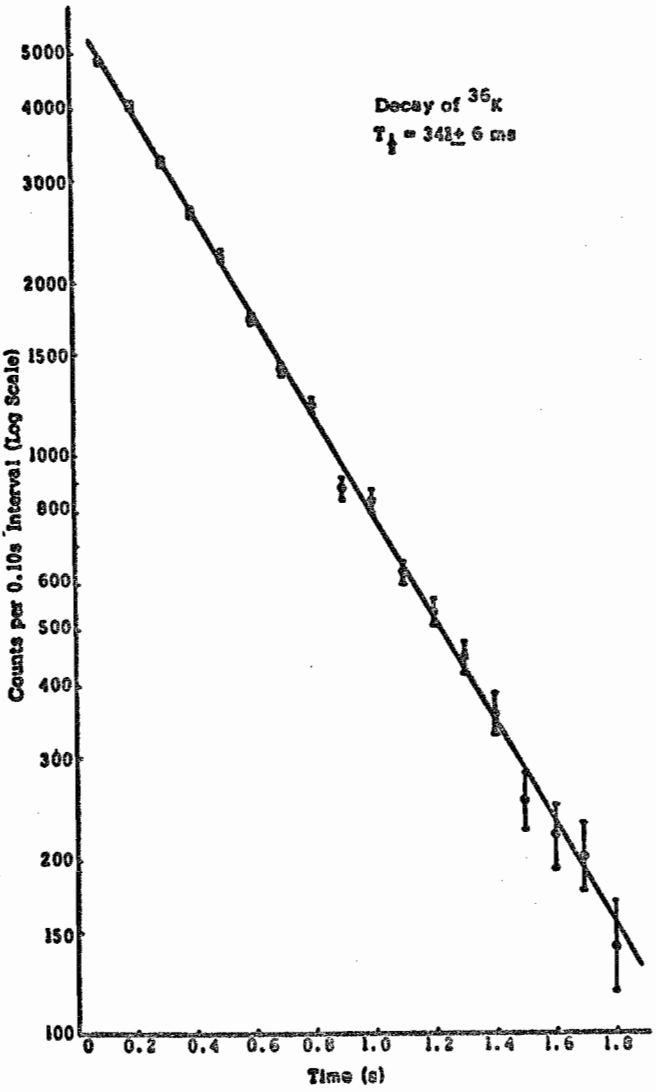

Figure 4.2 ^{36}K decay curve showing least-squares fit

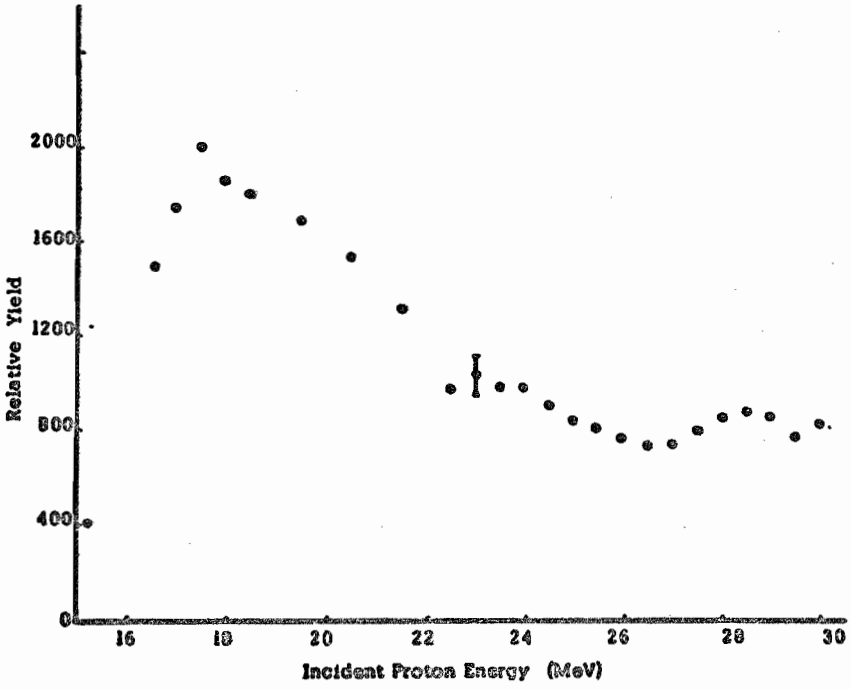

Figure 4.3 Observed excitation curve for positrons from $^{36}Ar(p,n)^{36}K$ for incident proton energies between 15 and 30 MeV

threshold were carefully examined using the decay analysis computer program to see if any decaying component other than that attributed to ^{36}K could be found. However, no new decay component could be distinguished.

4.2 $^{36}Ar(p,n)^{36}K$ Reaction Yield from Threshold to 15 MeV

Preliminary experimental work indicated that there was a considerable amount of structure in the $^{36}Ar(p,n)^{36}K$ yield curve for incident proton energies between threshold (14 MeV) and 15 MeV. Therefore, when the high-resolution beam energy analyzing system described in Section 3.2.3 became available, the reaction yield in this energy region was investigated in detail.

4.2.1 Experimental Procedure

As in the previous experiments, the reaction yield was determined by measuring the amount of positron activity having a decay-time characteristic of ^{36}K. The same detector, electronics, and calibration procedure that were employed for measuring the yield at higher energy were also used for this experiment. However, significant improvements in equipment and data processing were made.

One improvement for the high-resolution work was to use Kapton plastic film rather than tantalum foil for the gas cell window. This has the advantage of reducing the beam energy-loss and straggling, and may also produce less background. However, because Kapton is more easily

damaged by the beam, the intensity was kept below 50 nA in order to reduce the danger of breaking the cell. Another improvement was the use of an electrostatic beam chopper which was controlled by the computer. This arrangement had the advantage of greater timing versatility and precision. In addition to the computer program changes required for chopper control, the memory block allocated for data storage was doubled to 4096 locations. Consequently, 32 timed positron spectra of 128 channels each were recorded for each incident proton energy. The computer timing input parameters were selected to give a beam-on activation time of 0.30 s followed by a beam-off counting period of 3.2 s or about nine half-lives.

The proton energy was varied in steps as small as 50 keV between 14.0 and 15.5 MeV. Beam current varied between 30 and 50 nA, and the total collected charge was typically 2 μC for each proton energy.

4.2.2 Results

The ^{36}K yield was analyzed by first generating decay curves for each incident proton energy. These curves were created by summing over the positron energy range of 3 to 5 MeV in each timed spectrum. A least-squares fit to each decay curve was then made by holding the half-life parameter fixed at 341 ms, and allowing the amplitude parameters of the decay-component and background to vary. The amplitude parameters for the 341 ms component were then normalized with respect

to collected charge and plotted as a function of proton energy. The yield curve obtained in this way is plotted in Figure 4.4. The energy coordinates for points on the curve have not been adjusted for energy lost in passing through the gas cell window. This energy loss is about 85 keV for the range of proton energies shown.

4.3 Mass of ^{36}K

The mass of ^{36}K was determined from the threshold of the $^{36}Ar(p,n)^{36}K$ reaction by detecting the positron activity of ^{36}K. The absolute proton energy calibration was obtained by measuring the $^{32}S(p,n)^{32}Cl$ threshold using CS_2 vapor as a target in the same gas cell.

4.3.1 Experimental Procedure

The $^{36}Ar(p,n)^{36}K$ threshold experiment was performed during the same experimental period that the half-life and reaction yield above 15 MeV were measured. Therefore, the detector, electronics, and general procedure for setting up the experiment have been described in Section 4.1. Computer timing input and the rotational speed of the mechanical beam chopper were set to give a target activation time of about 1.0 s followed by a beam-off counting period of 2.0 s per chopper cycle. For the argon target, the energy of the proton beam was varied in 30 keV steps from 14.170 MeV to 14.500 MeV, accumulating 40 μC at each point.

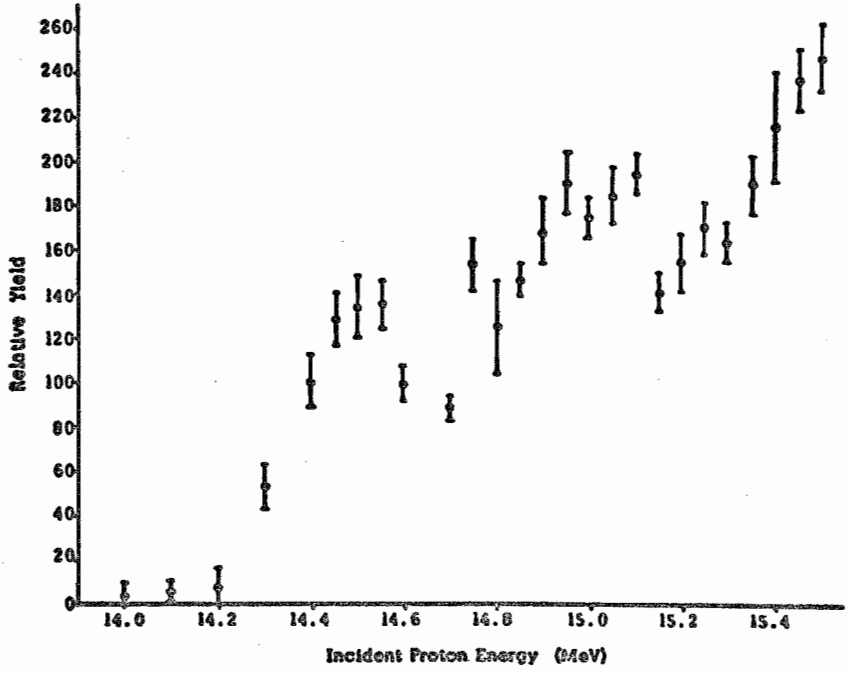

Figure 4.4 Observed excitation curve for positrons from $^{36}Ar(p,n)^{36}K$ for incident proton energies between 14 and 15 MeV

After finishing with the argon target, this gas was pumped out and replaced by a CS_2 vapor target. CS_2 is a volatile liquid at room temperature and pressure. Therefore, to introduce the vapor into the gas cell, a few drops were placed in a copper tube which was sealed at one end. This tube was then attached to the target gas system and the CS_2 quickly frozen by placing the end of the copper tube in liquid nitrogen. The target gas cell and piping were then pumped out with a vacuum pump while keeping the CS_2 frozen. The CS_2 was then allowed to warm up and vaporize producing a gas cell pressure of 1/2 atm.

According to Anderson et al. (1966), the half-life of ^{32}Cl is 294 ± 6 ms and positron branches having end-point energies of 9.22 MeV (60%), 7.17 MeV (2%), 6.76 MeV (7%), 5.91 MeV (6%), and 4.45 MeV (20%) were deduced from gamma-ray intensity measurements. Because these values are very close to those of ^{36}K, the same chopper timing and amplifier gain were used. Proton bombarding energy was varied in 10 keV steps between 14.10 and 14.20 MeV. The total beam charge collected for each proton energy was 40 μC.

4.3.2 Results

The yield near threshold from both the sulfur and argon targets was analyzed by the technique described in Section 4.2.2. A decay curve for each incident proton energy was generated by summing over an interval from 4.5 to 8.0 MeV in the timed ^{36}K positron spectra, and an

identical interval for the ^{32}Cl positron spectra. Least-squares fits to these decay curves were then used to determine the amount of activity having the proper time decay. The half-life of ^{32}Cl was found to be 302 ± 4 ms which is in good agreement with the previously published value. The yield near threshold for both reactions is shown in Figure 4.5. Proton energies for points on these curves have been adjusted for energy lost in the tantalum gas cell window. By measuring and weighing the foil, a thickness of 10.58 mg/cm^2 was found. The energy loss for Ta ($Z = 73$) was determined by extrapolating from Au ($Z = 79$) and Pb ($Z = 82$) energy losses using the graphs of Marion (1968). An energy loss of 160 keV was arrived at for 14 MeV protons, and this value varies by less than 1 keV over the proton energy range shown in Figure 4.5.

The yield near threshold was fit using least-squares analysis to the function

$$Y = 0 \quad \text{for } E \leq E_{th}$$

$$Y = A(E - E_{th})^{3/2} \quad \text{for } E_{th} < E < E_{th} + \Delta E_t$$

$$Y = A(E - E_{th})^{3/2} - (E - \Delta E_t - E_{th})^{3/2} \quad \text{for } E \geq E_{th} + \Delta E_t$$

where Y is the yield at proton energy E, E_{th} is the threshold energy, ΔE_t is the proton energy lost in passing through the target, and A is a proportionality factor. This function was derived by first finding the yield as a function of proton energy for an infinitely thin target, assuming that the cross section for (n,p) reactions is proportional to the reciprocal of neutron velocity for very low neutron energy, and that the

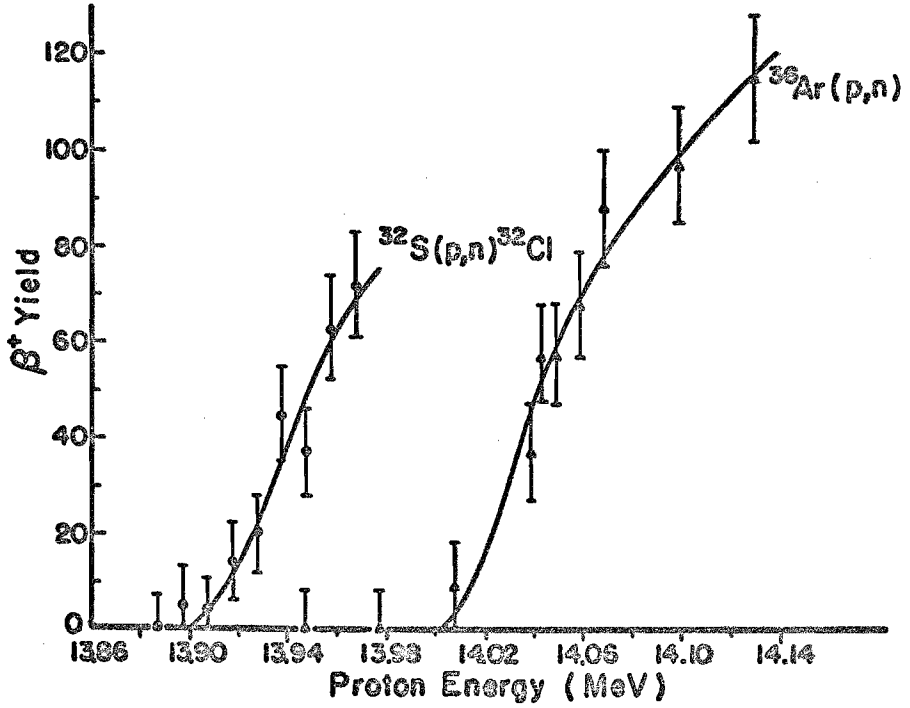

Figure 4.5 Observed excitation curves for positrons from $^{32}S(p,n)^{32}Cl$ and from $^{36}Ar(p,n)^{36}K$ near the reaction thresholds

cross section for the (p,n) reaction can then be found by using the reciprocity theorem for inverse reactions. The function giving the yield from a target of finite thickness was then found by integration. Target energy losses of 32 keV for argon and 48 keV for CS_2 gas were estimated using the graphs of Marion (1968).

The $^{32}S(p,n)^{32}Cl$ threshold was found at an incident proton energy of 13.900 ± 0.015 MeV which is in excellent agreement with a value of 13.899 ± 0.014 MeV published by Overley et al. (1969). The $^{36}Ar(p,n)^{36}K$ threshold was found 103 ± 20 keV higher, yielding a value of 14.002 ± 0.024 MeV for the threshold energy and a ground state Q-value of -13.618 ± 0.023 MeV for the reaction. Using the mass excess of ^{36}Ar(-30.2305 ± 0.0011 MeV) from the mass tables by Wapstra and Gove (1971)[1], the mass excess of ^{36}K is found to be -17.395 ± 0.023 MeV ($^{12}C = 0$).

All uncertainties given in the present work are estimated standard deviations. The uncertainties in the threshold energies take into account uncertainties in the least-squares fits, and in proton energy losses in the target cell window and target gases. The final uncertainty of the mass excess was found by combining the uncertainty of the threshold energy difference with the uncertainty of the $^{32}S(p,n)^{32}Cl$ threshold energy using the standard method for propagation of errors.

---

[1] To be published in Nuclear Data Tables 9:265-468

4.4 Excited States of ^{36}K

The level energies for 10 excited states in ^{36}K were measured by means of the $^{36}Ar(^{3}He,t)^{36}K$ reaction. Also, the energies of triton groups corresponding to the formation of ^{36}K in the ground state provide an additional measurement of the ^{36}K mass. The $^{14}N(^{3}He,t)^{14}O$ reaction was used for triton energy calibration.

4.4.1 Experimental Procedure

A 22.2 MeV ^{3}He beam from the tandem Van de Graaff was incident on an 2.5 cm gas cell centered in a 60 cm scattering chamber (see Figure 3.2). The outgoing particles were detected by a counter telescope which used a transmission detector 50 μm thick backed by a 1500 μm detector. Both were fully depleted silicon surface barrier detectors. A collimator consisting of a pair of slits 1.5 mm wide and 6 mm high spaced 6.3 cm apart was placed in front of the counter and 1-5/16 inch away from the target gas cell. Pulses from the two detectors were first amplified and then processed by the on-line computer using the mass-identification program. The gas cell, target chamber, and particle identification technique are described in detail in Chapter 3.

The triton spectra were calibrated using triton peaks of known energy from the $^{14}N(^{3}He,t)^{14}O$ reaction. A nitrogen gas target pressure of 1/2 atm was used, and the energy loss difference between the

nitrogen and argon targets was taken into account. Triton spectra from a 0.2 atm argon (99.9% ^{36}Ar) target were taken with detector angles of 30, 40, and 50 degrees. The intensity of the ^{3}He beam was typically 150 nA, and a total charge of 1600 μC was collected at each angle. A spectrum taken after removing the argon from the target cell showed that the background contribution was negligible.

4.4.2 Results

The triton spectra from both the $^{14}N(^{3}He,t)^{14}O$ and the $^{36}Ar(^{3}He,t)^{36}K$ reactions are shown in Figure 4.6. Each peak indicated in the spectrum from ^{36}Ar has the same nuclear reaction Q-value for mass 36 at each of the two or three angles at which the peak was observed. The excitation energies for levels in ^{36}K corresponding to each peak are listed in Table 4.1. The consistency of the energy determinations at the three angles was good. Therefore, the errors listed in Table 4.1 are primarily the result of uncertainties in the peak centroids.

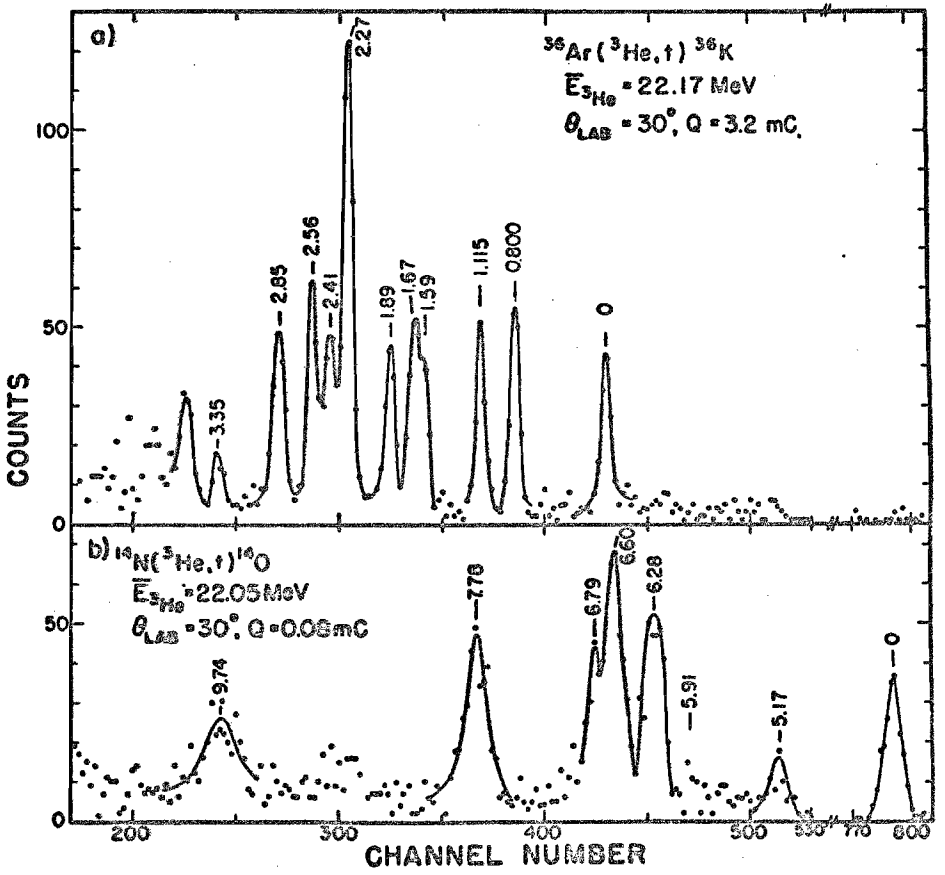

Figure 4.6 Energy spectra for (^{3}He,t) reactions on ^{14}N and ^{36}Ar gas targets with beam energies at the center of each target and the total beam charges indicated

Table 4.1 Energy levels in ^{36}K from present work

Level	Excitation Energy (MeV)
0	0
1	0.800 ± 0.015
2	1.115 ± 0.015
3	1.59 ± 0.02[a]
4	1.67 ± 0.02[a]
5	1.89 ± 0.02[a]
6	2.27 ± 0.02
7	2.41 ± 0.03
8	2.56 ± 0.03
9	2.85 ± 0.03
10	3.35 ± 0.04

[a]These states were observed only at scattering angles of 30° and 40°

4.5 Gamma-Ray Transitions in ^{36}Ar following the Positron Decay of ^{36}K

An 80 cc Ge(Li) detector was used to measure gamma-ray transitions in ^{36}Ar following from the decay of ^{36}K. Measurements of gamma-ray intensity measurements were used to calculate positron branching ratios.

4.5.1 Experimental Procedure

^{36}K was produced by the $^{36}Ar(p,n)^{36}K$ reaction using a chopped proton beam from the Cyclo-Graaff accelerator. A beam energy of 18 MeV was used because the reaction yield reaches a maximum value near that energy. (See Figure 4.3.) The beam was focused through a 1/8-inch diameter collimator into a target gas cell 5 inches long and 1/2 inch in diameter. The target cell contained argon (99.9% ^{36}Ar) at a pressure of 1/2 atm, and was sealed with 0.001 inch Kapton plastic film. After passing through the target, the beam was stopped 6 feet away in a thick carbon block. The detector was calibrated with a ^{56}Co gamma-ray source, and the amplifier gain set so that gamma-rays with an energy range of 0 to 8 MeV could be recorded. The chopper speed and computer timing were adjusted to give a beam-on activation period of 1/6 s and a counting period of 2/3 s per chopper cycle.

The experiment was divided into two main parts. In the first part, a single 4096-channel gamma spectrum was taken with a wide dispersion of about 2 keV per channel. This was done to achieve the best possible energy resolution and separation of closely spaced peaks. Approximately 12 hours were required to collect this data using a proton beam current of about 20 nA. In the second part of the experiment, the computer was set to accumulate four timed gamma spectra of 1024 channels each. Each spectrum was allowed to accumulate for 1/6 second starting at a precisely timed instant after target activation had

ceased. By this procedure, the time decay of peaks in the spectrum could be measured allowing gamma rays originating from the decay of ^{36}K to be identified. These spectra also required an acquisition time of about 12 hours. As an additional check on background activity, a 4096-channel spectrum was taken with the argon removed from the target gas cell.

4.5.2 Results

The wide dispersion spectrum is shown in Figures 4.7 and 4.8. Peaks identified as originating from ^{36}Ar as well as prominent contamination peaks have been labeled. Four background peaks for which the energy is well known served as convenient gamma-ray energy calibration points. The full-energy, first escape, and second escape peaks from the decay of ^{14}O (71-second half-life) produced by the $^{14}N(p,n)^{14}O$ reaction gave calibration points at 2312.7 $\pm$ 0.10 keV, 1801.7 $\pm$ 0.10 keV, and 1290.7 $\pm$ 0.10 keV respectively. Nitrogen is an element contained in the Kapton window material. The fourth calibration point was from the decay of ^{24}Na (2753.9 $\pm$ 0.12 keV gamma-ray energy) which is a part of the target room background. A least-squares straight line through the four points provided the final calibration curve. A linear function was chosen because no statistically significant deviation from linearity could be observed in the peak positions of the ^{56}Co spectrum. An off-line computer analysis, consisting of peak centroid and area

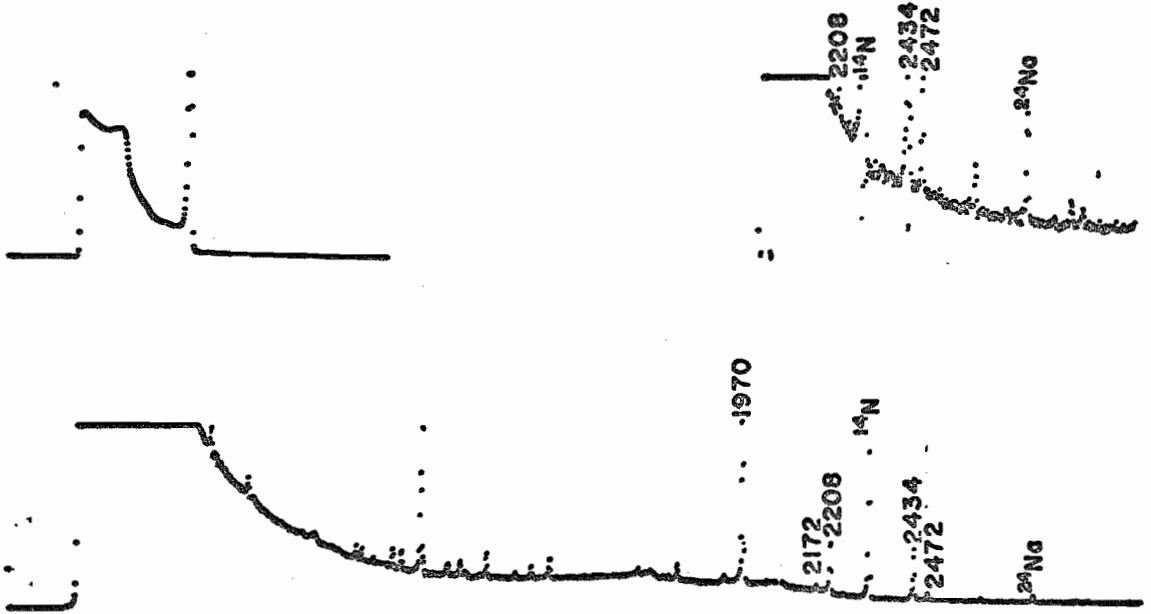

Figure 4.7 First 2048 channels of the delayed gamma-ray spectrum from $^{36}Ar(p,n)^{36}K$ showing ^{36}Ar gamma-ray energies in keV and prominent contamination peaks (upper figures have different vertical scale to show detail)

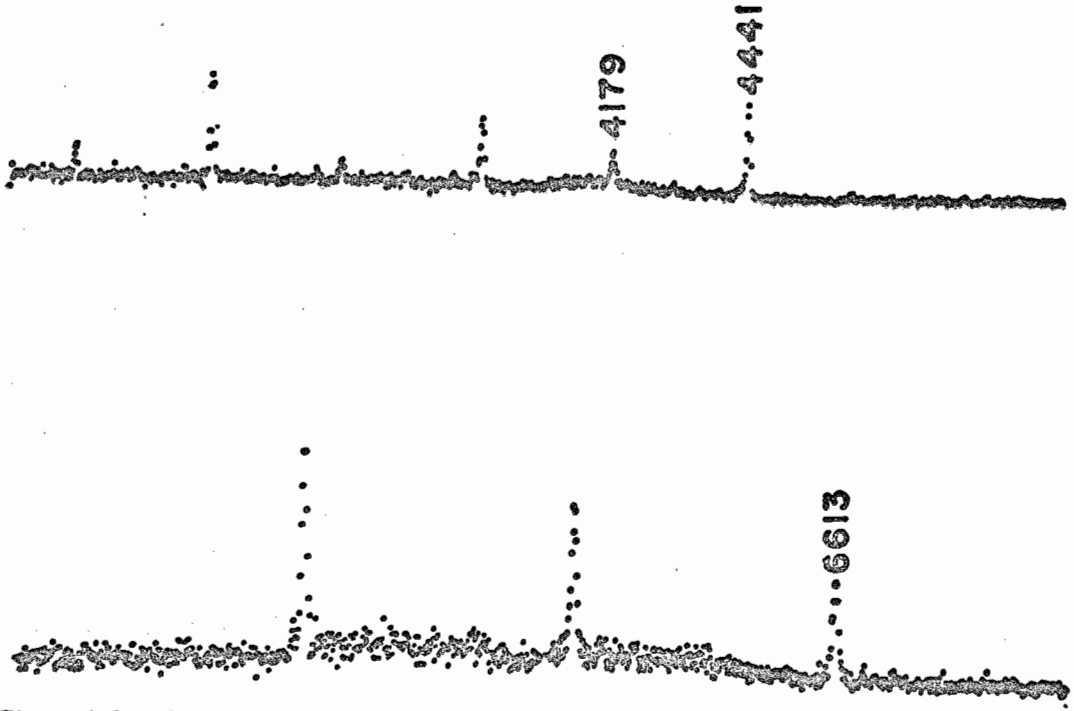

Figure 4.8 Channels 2049 – 3072 (upper) and channels 3073 – 4096 (lower) of the delayed gamma-ray spectrum from $^{36}Ar(p,n)^{36}K$ showing ^{36}Ar gamma-ray energies in keV (unlabeled peaks are escape peaks)

determinations after straight-line background subtraction, was performed on each spectrum. The uncertainty in the energy corresponding to each peak was determined by combining the standard deviation of the centroid with the standard deviations of the slope and intercept parameters of the straight-line fit through the calibration points. The final gamma-ray energy and uncertainty for each ^{36}Ar transition were then found by a weighted average between the full-energy peak and the escape peaks. The relative intensities of the gamma rays were determined from the peak areas using the known detector efficiency. The energies and intensities are listed in Table 4.2. The intensities listed in the table are normalized to the number of ^{36}K disintegrations.

Table 4.2 Gamma-ray energies and intensities from present work

Energy (keV)	Relative Intensity
1969.8 ± 0.5	0.790 ± 0.080
2171.5 ± 0.9	0.022 ± 0.005
2208.3 ± 0.4	0.290 ± 0.040
2433.7 ± 0.4	0.330 ± 0.040
2472.0 ± 0.8	0.044 ± 0.007
4180.4 ± 1.0	0.031 ± 0.007
4441.7 ± 0.6	0.093 ± 0.005
4643.7 ± 1.4	<0.009
6612.7 ± 0.8	0.073 ± 0.009

The four timed gamma spectra were also computer-analyzed to obtain the peak areas and centroids. The areas were then corrected to account for relative dead time between the four spectra by normalizing to the area of the 2312.7 keV ^{14}N contamination peak. The time-decay of the corrected areas was then analyzed using the decay-analysis computer program. Thus, each peak having the decay-behavior characteristic of ^{36}K was identified. The results of this analysis are shown in Figure 4.9 which shows the least-squares fit through the four data points obtained by keeping the half-life parameter fixed at the value corresponding to ^{36}K.

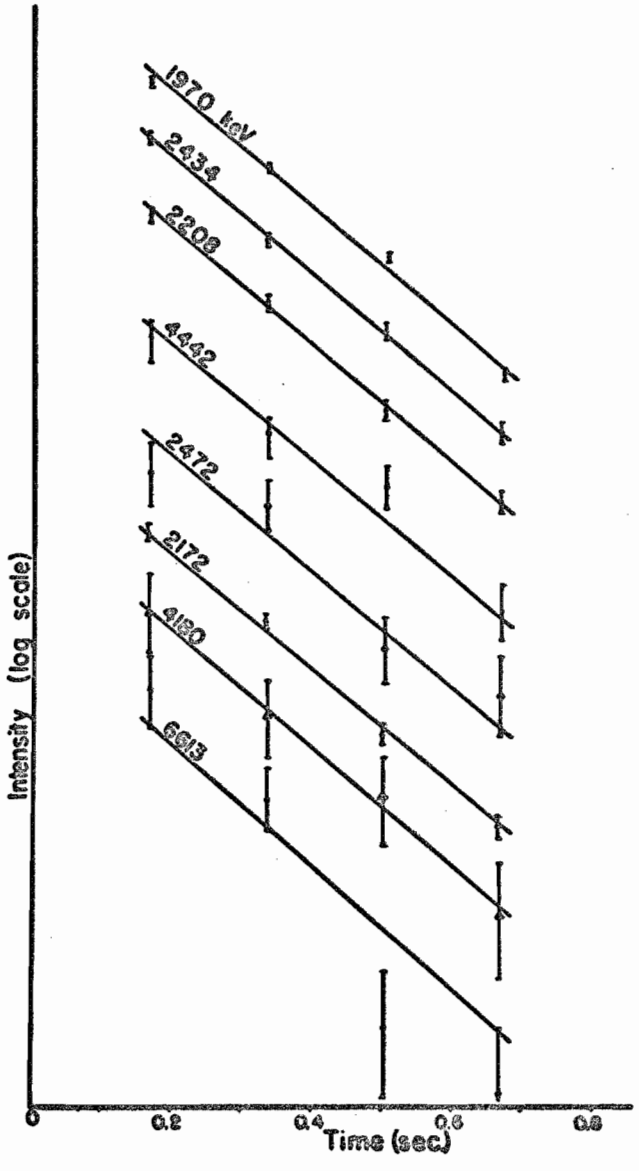

Figure 4.9 Decay curves for gamma rays arising from transitions in ^{36}Ar following the decay of ^{36}K showing the best 341 ms fits to the data

5. DISCUSSION AND CONCLUSIONS

5.1 Mass of ^{36}K

Two independent determinations of the ^{36}K mass have been made. A mass excess of -17.395 ± 0.023 MeV was obtained from the $^{36}Ar(p,n)^{36}K$ reaction threshold, and -17.32 ± 0.04 MeV was found from the $^{36}Ar(^{3}He,t)^{36}K$ reaction Q-value. This leads to a final weighted average of -17.38 ± 0.03 MeV where the external uncertainty as defined by Birge (1932) is used. This value is compared to previously reported work in Table 5.1 and with a preliminary value found by Alburger (1970)[1] after the present work had been completed.

Table 5.1 Comparison of ^{36}K mass determinations

Mass Excess (MeV)	Origin
-17.38 ± 0.03	Present work.
-17.388	Preliminary value from Alburger from the $^{36}Ar(p,n)^{36}K$ reaction threshold.
-17.33	Prediction by Berg et al. (1967) using the excitation energy of the first T = 1 state in ^{36}Ar and an estimation of the ^{36}Ar - ^{36}K Coulomb energy difference.
-17.42 ± 0.05	Prediction by Kelson and Garvey (1966) from a parameterless mass equation for proton-rich nuclei.
-15.58	Experimental determination by Matlock (unpublished) using the $^{36}Ar(^{3}He,t)^{36}K$ reaction Q-value.

[1]Private communication from David Alburger, Brookhaven National Laboratory, Upton, New York.

The energy of the first T = 1 excited state in ^{36}Ar has been determined from gamma-ray energy measurements. This experiment was first performed by Berg et al. (1967) and repeated in the present work (see Sections 4.5 and 5.4). Using this excitation energy and the ^{36}K mass, the ^{36}Ar - ^{36}K Coulomb-displacement energy is found to be 7.02 ± 0.03 MeV. This value fills a gap in the available data on Coulomb-displacement energies between the T_z = 0 and T_z = -1 members of the T = 1 isospin triplets which have now all been measured up to A = 42.

The present value is in good agreement with systematics of Coulomb-displacement energies of other studies in this mass region which are plotted in Figure 5.1. With the exception of the present value and that for A = 32, the values plotted in Figure 5.1 are taken from Jänecke (1970). A value of 6.473 ± 0.014 MeV for the Coulomb-displacement energy of ^{32}S - ^{32}Cl was deduced using the ^{32}S(p,n)^{32}Cl threshold measurement of Overley et al. (1969). In Figure 5.1, the trend of the lower curve is expected to be generally parallel to the upper curve if shifted by two mass units to the left. The two striking exceptions to this rule are now evident. They occur at A = 14 - 16 and A = 38 - 40 and are thought to be due to shell-closure effects.

The present study of the ^{36}K mass has been published by Jaffe et al. (1971).

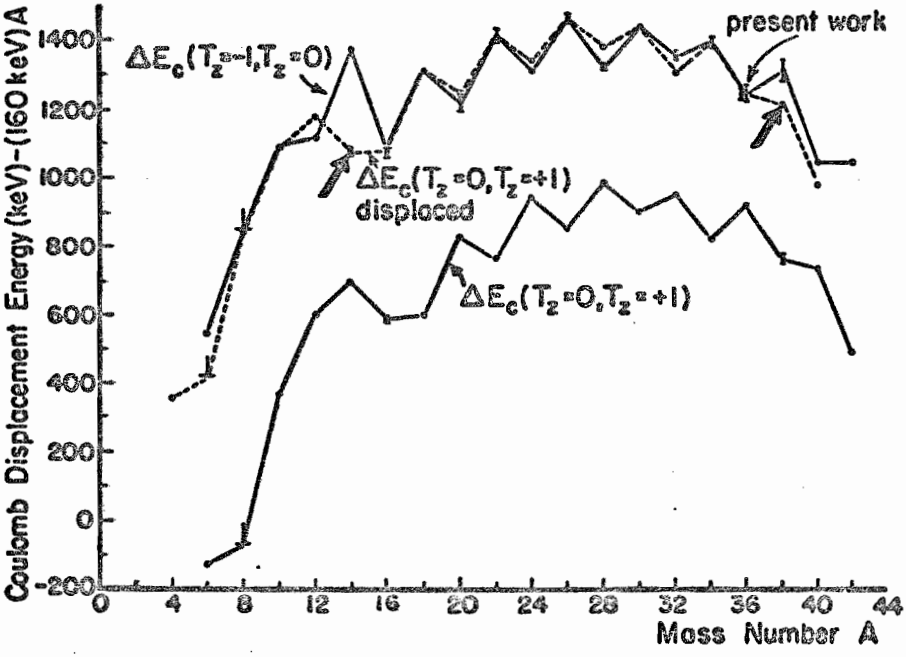

Figure 5.1 Coulomb-displacement energy between the two adjacent members of T = 1 triplets versus mass number with a linear sequence (160 keV)A subtracted in order to eliminate the steep rise. Dashed line represents the lower trend after displacement of two mass units to the left and an upward shift as to coincide with the upper trend

5.2 Decay Properties of ^{36}K

The half-life of ^{36}K was found to be 341 ± 6 ms. This value was determined by timing the positron activity following the $^{36}Ar(p,n)^{36}K$ reaction. The value found is 76 ms larger than the 265 ± 25 ms reported by Berg et al. (1967) but carries a considerably smaller uncertainty. The half-life found in the present work agrees very well, however, with the value of 336 ± 4 ms found by Alburger (1970)[1] after the completion of the present work.

A careful study was made of gamma transitions in ^{36}Ar following the decay of ^{36}K. Eight gamma rays having a decay time corresponding to ^{36}K were found. A ninth gamma ray with an energy of 4643.7 ± 1.4 keV was observed, and is thought to arise from the transition between the 6613 keV 2^+ level and the 1970 keV 2^+ level of ^{36}Ar. The intensity of this peak was too small to establish the decay time. However, a measurement of its intensity in the wide-dispersion spectrum (see Section 4.5) shows that this transition cannot account for more than about 0.4% of the gamma decay from the 6613 keV level. This low value is surprising since a lower energy transition to the 4441 keV 2^+ level was observed with a 5% branching ratio. The energies of these transitions are listed and compared with previous work in Table 5.2.

---

[1]Private communication from David Alburger, Brookhaven National Laboratory, Upton, New York.

Table 5.2 Gamma transitions in ^{36}Ar following the decay of ^{36}K

Gamma Ray Energies (keV)		
Present Work	Previously Published Values	
1969.8 ± 0.5	1970.0 ± 0.7	Berg et al. (1967)
2171.5 ± 0.9	None	
2208.3 ± 0.4	2206.7 ± 1.0	Berg et al. (1967)
2433.7 ± 0.4	2434.4 ± 0.7	Berg et al. (1967)
2472.0 ± 0.8	2460 ± 20	Erne and Endt (1965)
4180.4 ± 1.0	4178.3 ± 0.9	Berg et al. (1967)
4441.7 ± 0.6	4439.8 ± 1.2	Berg et al. (1967)
4643.7 ± 1.4	None	
6612.7 ± 0.8	6609.6 ± 2.0	Berg et al. (1967)

The gamma-ray energies were combined and corrected for recoil to give the ^{36}Ar level energies shown in Table 5.3.

Table 5.3 Energy levels of ^{36}Ar (keV)

Present Work	Values from Endt and van der Leun (1967)	Weighted Averages
1969.9 ± 0.5	1970.1 ± 0.7	1970.0 ± 0.4
4178.6 ± 1.1	4177.9 ± 0.7	4178.1 ± 0.6
4442.0 ± 0.5	4440.1 ± 1.2	4441.7 ± 0.7
6613.3 ± 0.6	6611.9 ± 0.9	6612.9 ± 0.6

The relative intensities of the gamma rays were measured (see Table 4.2) and used to deduce the branching ratios of positron branches to three levels in ^{36}Ar. The branching ratios and the ^{36}K half-life were then used to calculate a log ft value for each positron branch using the table by N. B. Gove[1]. A log ft of 3.49 was found for the positron branch to the 6.613 MeV level in ^{36}Ar verifying that this state is the analog of the ^{36}K ground state. For the other two positron branches, log ft values of about 4.8 were found which is in good agreement with theory and systematics for allowed transitions.

The results of the study are summarized in the decay diagram of Figure 5.2, and descriptions of this work have been published by Jaffe et al. (1971) and by Miller et al. (1971).

5.3 Energy Levels in ^{36}K

The ground state and 10 excited states in ^{36}K have been observed by means of the ^{36}Ar(^{3}He,t)^{36}K reaction. The excitation energies for these states have been listed in Table 4.1. The Q-value for the reaction exciting the ground state of ^{36}K was determined to be -12.93 $\pm$ 0.04 MeV leading to the ^{36}K mass excess of -17.32 $\pm$ 0.04 MeV. This is in fair agreement with the ^{36}K mass excess of -17.395 $\pm$ 0.023 MeV determined from the ^{36}Ar(p,n)^{36}K reaction threshold (Section 5.1).

---

[1]To be published in Nuclear Data Tables.

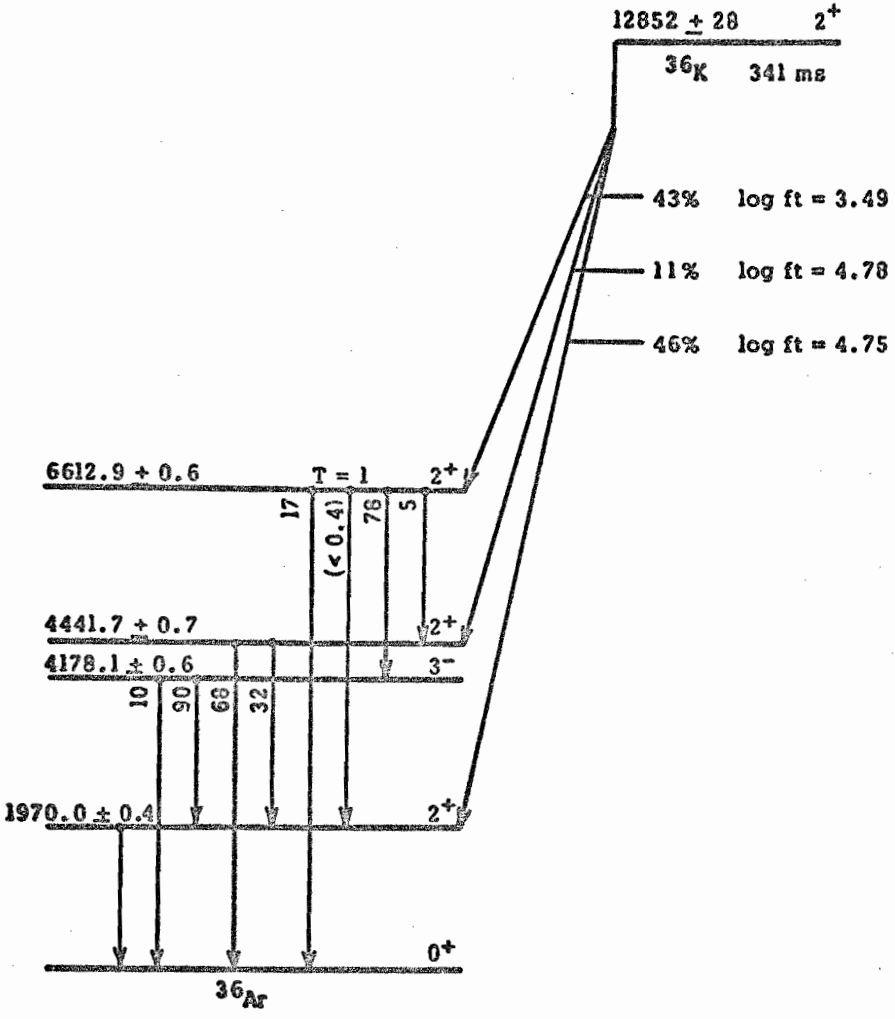

Figure 5.2 Decay diagram for ^{36}K showing gamma transitions in ^{36}Ar

The excitation energies obtained for the states of ^{36}K are compared in Figure 5.3 to those of the analog nucleus ^{36}Cl as cited by Endt and van der Leun (1967). The energies of the first three excited states of ^{36}K agree within 50 keV with the corresponding levels of ^{36}Cl. The level observed in the present work at an excitation energy of 1.67 MeV in ^{36}K is 0.29 MeV below the next excited state in ^{36}Cl. It appears significant that of the doublet at 1.949 and 1.957 MeV in ^{36}Cl, the latter is the lowest negative-parity state. The low-lying positive parity states of ^{36}Cl have configurations predicted from the shell model to be $(1d_{3/2})_p (1d_{3/2})_n^3$, with probable admixtures involving holes in the $2\,s_{1/2}$ and $1d_{5/2}$ shells. The negative parity state may be assumed to be the result of the excitation of a single particle into the $1f_{7/2}$ shell. Thus, a possible wave function for a low-lying odd-parity state in ^{36}Cl is $(1f_{7/2})_n (1d_{3/2})_n^2 (1d_{3/2})_p$ with that of the analog state in ^{36}K given by $(1f_{7/2})_p (1d_{3/2})_p^2 (1d_{3/2})_n$. The promotion of a single proton from the $1d_{3/2}$ shell into the $1f_{7/2}$ shell can lead to a downward energy shift of about 250 keV as seen from Coulomb energies for nuclear ground states according to Jänecke (1970). This can be explained by the fact that the Coulomb interaction of a proton in an outer shell with protons in inner shells is less than that between protons in the same shell. This effect has been mentioned by Harchol et al, (1967). In addition, the electromagnetic spin-orbit interactions for $1f_{7/2}$ and $1d_{3/2}$ protons are estimated by Nolen and Schiffer (1969) to be -106 and +114 keV,

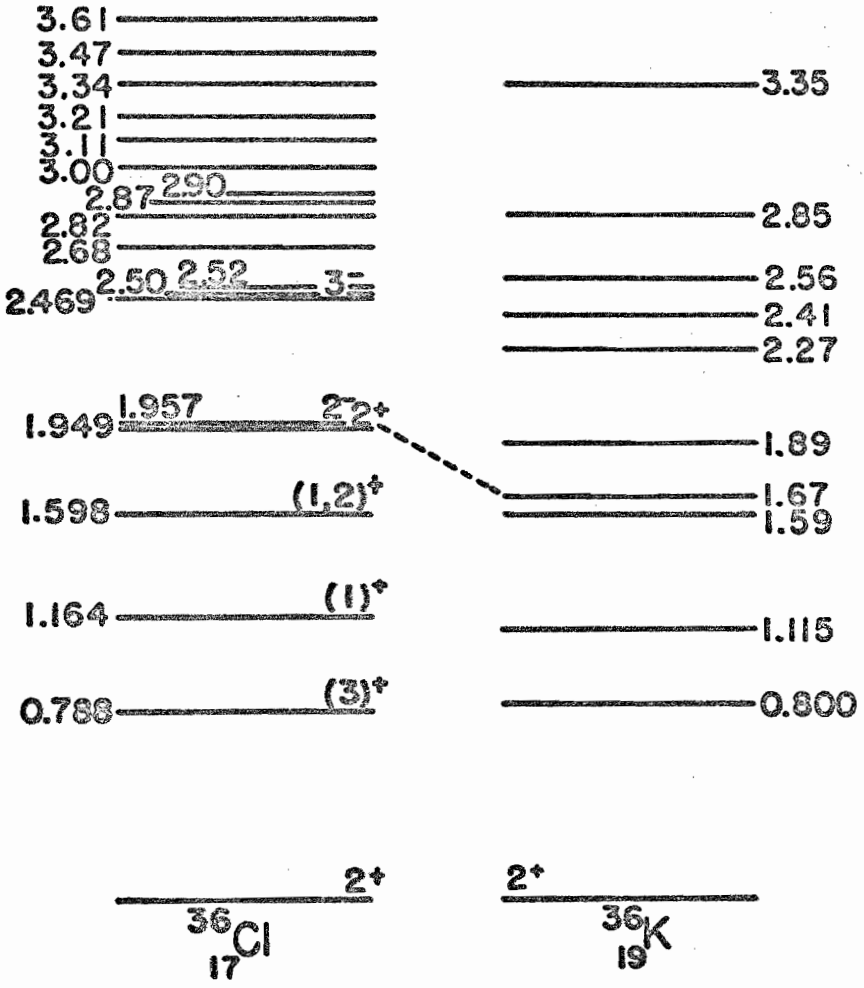

Figure 5.3 A comparison of levels in ^{36}Cl and ^{36}Ar

respectively, giving a net downward shift due to the spin-orbit term of 220 keV. The above argument implies that the 1.67 MeV level (or possibly the 1.59 MeV level) of ^{36}K is the analog of the 1.957 MeV 2^- state in ^{36}Cl, and the 1.89 MeV level in ^{36}K is the analog of the 1.949 MeV 2^+ level of ^{36}Cl.

The present study of the excited states of ^{36}K has been published by Dzubay et al. (1970).

5.4 Excitation Function for the $^{36}Ar(p,n)^{36}K$ Reaction

The positron yield following the $^{36}Ar(p,n)^{36}K$ reaction has been measured using a chopped proton beam with incident proton energies varying from the reaction threshold (14 MeV) to 30 MeV. The yield between 14 and 15 MeV was examined very carefully using a high-resolution beam energy analyzing system. This was done in order to obtain the details of structure observed in the excitation function for that energy range. This portion of the excitation curve is plotted in Figure 4.4, and shows sharp rises or peaks in the yield about 14.4 and 14.8 MeV. If these were additional thresholds, they would correspond to excited states of ^{36}K at about 0.4 MeV and 0.8 MeV respectively. This might account for the higher energy peak since a ^{36}K level at 0.800 MeV was found using the $^{36}Ar(^3He,t)^{36}K$ reaction. However, this explanation cannot be used to describe the lower energy peak.

The structure of the excitation curve in this region may be largely due to effects in the compound nucleus ^{37}K. While T = 1/2 resonances would hardly be expected at this energy due to the high density of T = 1/2 states, there is the possibility of effects due to T = 3/2 resonances corresponding to analogs of states of ^{37}Ca at approximately 11 MeV excitation. According to Endt and van der Leun (1967), a resonance corresponding to the analog of the ground state of ^{37}Ca has been observed in the ^{36}Ar + p system with a proton energy of 3.06 MeV. However, these states will also have a fairly high density. On the other hand, according to Endt and van der Leun (1967), the first T = 5/2 state has been identified in ^{37}Cl at 10.24 MeV, and in ^{37}K it should have a similar spacing from the T = 3/2 state as it has from the ground state in ^{37}Cl. Hence, it should occur at an excitation of 15.3 $\pm$ 0.5 MeV in ^{37}K. Allowing for the center-of-mass correction and our gas cell window, we form ^{37}K at this excitation at an incident proton energy of about 13.9 $\pm$ 0.5 MeV on ^{36}Ar. Thus, the structure apparent in the positron yield curve (Figure 4.4) between 14 and 15 MeV may be caused by the presence of T = 5/2 resonances which would be well separated at this energy. These could not be formed directly by the addition of a proton (T = 1/2) to ^{36}Ar (T = 0) if they were of pure isospin, but they undoubtedly are mixed with the states of lower T. T = 2 resonances have been observed by Snover et al. (1969) by scattering alpha particles on ^{24}Mg although this process is doubly isospin

forbidden in both the entrance and exit channels. In the present case, the outgoing neutron would be only singly-isospin forbidden, a fact that could lead to a larger width for the resonances than in the above case.

Figure 4.3 shows the excitation curve for incident proton energies between 15 and 30 MeV. This curve rises to a sharp maximum at a proton energy of 17.5 MeV and then drops. The decreasing yield may be the result of increased competition from the (p,d) and (p,np) reactions which become energetically possible for proton energies of 13.55 MeV and 15.78 MeV, respectively.

5.5 Suggestions for Future Experimentation

5.5.1 Excited States of ^{36}K

Nothing is known about the spins and parities of levels in ^{36}K other than what can be inferred from levels in the analog nucleus ^{36}Cl. Therefore, a more extensive experiment using the $^{36}Ar(^{3}He,t)^{36}K$ reaction in which angular distributions of the triton groups are measured would be useful. In addition, a study of the prompt gamma spectrum during the $^{36}Ar(p,n)^{36}K$ reaction could yield information about the characteristics of states in ^{36}K by using gamma-ray angular distributions. An experiment of this type could also improve level energy determinations by making accurate gamma-ray energy measurements.

5.5.2 $^{36}Ar(p,n)^{36}K$ Excitation Curve

A detailed explanation of the shape of the (p,n) excitation curve might be possible after a study of the excitation functions of other proton-induced reactions on ^{36}Ar such as (p,p) or (p,p'). Such information is completely lacking at the present time for incident proton energies in the range of interest.

6. LIST OF REFERENCES

Anderson, W. C., L. T. Dillman, and J. J. Kraushaar. 1966. The Decay of ^{32}Cl and ^{40}Sc and the T = 1 Isobaric Analogue States in ^{32}S and ^{40}Ca. Nuclear Physics 77:401 - 424.

Berg, R. E., J. L. Snelgrove, and E. Kashy. 1967. ^{36}K Decay and T = 1 Analog in ^{36}Ar. Physical Review 153: 1165 - 1168.

Birge, R. T. 1932. The Calculation of Errors by the Method of Least Squares. Physical Review 40: 207 - 227.

Dzubay, T. G., A. A. Jaffe, E. J. Ludwig, T. A. White, F. Everling, D. W. Miller, and D. A. Outlaw. 1970. Energy Levels of ^{36}K. Physics Letters 33B: 302 - 304.

Endt, P. M., and C. van der Leun. 1967. Energy Levels of Z = 11 - 21 Nuclei (IV). Nuclear Physics A105: 1 - 488.

Erne, F. C., and P. M. Endt. 1965. Levels of ^{36}Ar Excited in the $^{35}Cl(p,\gamma)^{36}Ar$ Reaction. Nuclear Physics 71: 593 - 605.

Goulding, F. S. 1964. A New Particle Identifier Technique for Z = 1 and Z = 2 Particles in the Energy Range $\geq$ 10 MeV. IEEE Trans. Nucl. Sci. NS - 11 (3): 388.

Harchol, M., A. A. Jaffe, J. Miron, I. Unna, and J. Zioni. 1967. The Coulomb-Displacement Energies of Nuclei. Nuclear Physics A90: 459 - 472.

Jaffe, A. A., G. A. Bissinger, S. M. Shafroth, T. A. White, T. G. Dzubay, F. Everling, D. W. Miller, and D. A. Outlaw. 1971. Mass and Half-Life of ^{36}K. Physical Review 3C: 2489 - 2491.

Jänecke, J. 1970. Isospin in Nuclear Physics, Chapter 8, edited by D. H. Wilkinson, published by North Holland Publishing Company, Amsterdam.

Kelson, I., and G. T. Garvey. 1966. Masses of Nuclei with Z $>$ N. Physics Letters 23: 689 - 692.

Marion, J. B., and F. C. Young. 1968. Nuclear Reaction Analysis, Chapter 1, published by North Holland Publishing Company, Amsterdam.

Matlock, R. G. 1965. The Study of Nuclear Coulomb-Energy Systematics. Unpublished PhD thesis, Department of Physics, University of Colorado, Boulder. University Microfilms, Ann Arbor, Michigan.

Miller, D. W., D. A. Outlaw, F. Everling, T. G. Dzubay, G. A. Bissinger, and S. M. Shafroth. 1971. Decay of ^{36}K. Bulletin of the American Physical Society 16: 554.

Nolen, J. A., and J. P. Schiffer. 1969. Coulomb Energies. Ann. Rev. of Nuc. Sci. 19: 471 - 526.

Overley, J. C., D. A. Bromley, and P. D. Parker. 1969. The Energy Calibration of Tandem Accelerators. Nuclear Instruments and Methods 68: 61 - 69.

Snover, K. A., D. W. Heikkinen, F. Riess, H. M. Kuan, and S. S. Hanna. 1969. Lowest T = 2 Level in ^{28}Si Observed as a Highly Forbidden Compound Nucleus Resonance in $^{24}Mg + \alpha$ Reactions. Physical Review Letters 22: 239 - 241.